



ELSEVIER

Computer Physics Communications 115 (1998) 18–24

Computer Physics
Communications

Wavelet-distributed approximating functional method for solving the Navier–Stokes equation

G.W. Wei^a, D.S. Zhang^a, S.C. Althorpe^a, D.J. Kouri^a, D.K. Hoffman^b

^a *Department of Chemistry and Department of Physics, University of Houston, Houston, Texas 77204-5641, USA*

^b *Iowa State University, Ames, IA 50011, USA*

Received 4 September 1998

Abstract

The Navier–Stokes equations with both periodic and non-slip boundary conditions are solved using a new class of wavelets based on distributed approximating functionals (DAFs). Extremely high accuracy is found in our wavelet-DAF integration of the analytically solvable Taylor problem, using 32 grid points in each of the two spatial dimensions, for Reynolds numbers from $Re = 20$ to $Re = \infty$. The present approach is then applied to the lid-driven cavity problem with standard non-slip boundary conditions. Physically reasonable solutions are obtained for Reynolds numbers as high as 3200, using 63 grid points in each spatial dimension. Our results indicate that wavelet methods are readily applicable to those dynamical problems for which the existence of possible singularities demands highly accurate solution methods. © 1998 Elsevier Science B.V.

PACS: 02.70.Rw; 02.30.Mv; 02.60.-x; 52.35.Mw

1. Introduction

In statistical mechanics, nonlinear partial differential equations (NPDEs) often arise when only part of the degrees of freedom in a physical system are accounted for explicitly. Since this is the standard approach in treating macroscopic systems, such equations are ubiquitous in the physical sciences and engineering. There are no general analytical solutions to most NPDEs of interest. Further, despite extensive efforts, finding numerical solutions for such equations is still a challenge because of the possible existence of singularities and/or homoclinic orbits that can induce instabilities or sharp transitions between different regions of “solution space” [1]. These difficulties can occur in many physical systems, including black holes in astronomy, shock waves in fluid flow, vortex sheets

in high Reynolds number incompressible fluid flow, and burst events in wall regions of turbulent boundary layers. Computational difficulties associated with these phenomena typically result from changes occurring over a broad range of spatial scales. The presence of these features can cause difficulties for numerical algorithms and can lead to numerically induced spatial and/or temporal chaos [2].

The Navier–Stokes equations provide an especially important example because of their wide applicability to modelling such diverse phenomena as weather, aerodynamic flow, chemical reacting flows, etc. These phenomena typically depend critically on complicated boundary conditions which in themselves can lead to very rich multiscale behavior of a flow. Complicated boundary conditions create difficulties for global basis set expansion methods. Consequently,

the most widely used solution techniques for solving the Navier–Stokes equations are local, such as finite difference or finite elements methods. However, these can encounter difficulties in delivering sufficiently accurate spatial derivatives, especially in regions of transition in scale lengths.

Recently, attention has been given to using wavelets [3–13] for this purpose because of their localized character in either Fourier or physical space. However, to date these attempts have not fulfilled their initial promise. In our view, there are two major difficulties in applying wavelet methods to solve the Navier–Stokes equations. The first is that treating complicated boundaries, while simultaneously carrying out a multiresolution analysis, has proved problematic. The second difficulty is that most existing wavelets are *not* smooth and rapidly decaying in both the physical and Fourier domains. These include wavelet systems such as the Haar, Shannon, Meyer, Daubechies and Battle–Lemarié wavelets [14–16]. An exception is the Gaussian family of “wavelets” [16], which do have optimal smoothness and localization in both physical and Fourier spaces. However, it is costly to achieve high accuracy using these.

Recently, Hoffman, Kouri and coworkers [17–21] have developed alternative methods based on distributed approximating functionals (DAFs) and have successfully applied them to a variety of computational problems (e.g., linear and nonlinear PDEs, signal processing, and various manipulations of experimental data). DAFs have been shown to have mathematical properties in common with wavelet “scaling functions” and have been used to create families of wavelets. We refer to these DAF scaling functions as wavelet-DAFs, and the associated (mother) wavelets as DAF-wavelets [22,23,25]. These are infinitely smooth and well localized in both physical and Fourier spaces. Furthermore, by appropriate choice of DAF parameters, they can be made arbitrarily close to ideal band-pass filters [19,22,24]. To date, DAFs have in general been used without recourse to multiresolution analysis, by simply tuning the DAF parameters to yield any desired (e.g., machine) accuracy [22,24–28]. All of the calculations in this study also focus on achieving high accuracy, without making use of multiresolution analysis. Taking advantage of the multiresolution capabilities of wavelet-DAFs is, of course, still an important and challenging problem

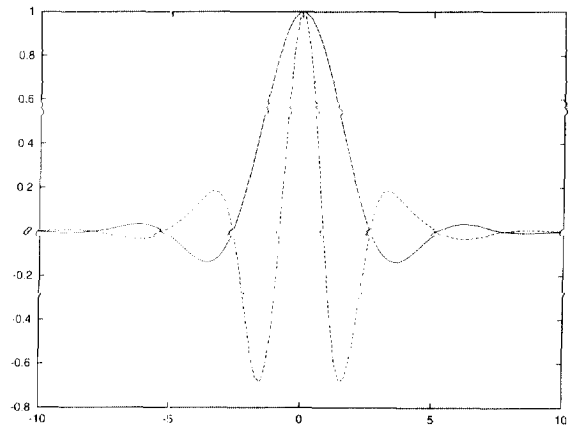


Fig. 1. The Shannon–Gabor-DAF wavelet. Solid line: the wavelet-DAF; dashed line: the DAF-wavelet.

which we will address in future work. In this regard, wavelet-DAFs show substantial promise because one can work solely in the physical space with guaranteed localization and smoothness in Fourier space.

This paper is organized as follows. In Section 2 we give the expressions for discretizing the NPDEs, and briefly discuss the numerical algorithm. Results of applications are discussed in Section 3 and Section 4 contains our conclusions.

2. Numerical algorithms

The Shannon–Gabor wavelet-DAF (in 1-D) is given by [23]

$$\delta_{\text{SGWD}}(x - x_k) = \frac{\sin \left[\frac{\pi}{\Delta} (x - x_k) \right]}{\frac{\pi}{\Delta} (x - x_k)} e^{-(x-x_k)^2/2\sigma^2}, \quad (1)$$

where Δ is the grid spacing and σ is a scale parameter. These wavelet-DAFs have optimal time-frequency localization as well as both smoothness and rapid decay properties (see Fig. 1). The n th order derivative operator is generated by

$$\delta_{\text{SGWD}}^{(n)}(x - x_i) = \frac{d^n}{dx^n} \left[\frac{\sin \left[\frac{\pi}{\Delta} (x - x_i) \right]}{\frac{\pi}{\Delta} (x - x_i)} \times e^{-(x-x_i)^2/2\sigma^2} \right]. \quad (2)$$

The wavelet-DAF approximation to a function and its n th derivative are given by appropriate convolutions,

which in the trapezoidal rule quadrature approximation are given by

$$F(x) \approx \sum_{i=-W}^W \delta_{\text{SGWD}}(x - x_i) F(x_i) \quad (3)$$

and

$$F^{(n)}(x) \approx \sum_{i=-W}^W \delta_{\text{SGWD}}^{(n)}(x - x_i) F(x_i), \quad (4)$$

where the kernel is banded, with total bandwidth $2W + 1$, because of the rapid Gaussian decay. For the two-dimensional flow problems we consider, we simply employ a direct product of DAFs in x and y . (There are generalizations of the DAF-wavelets that treat multi-dimensional problems without assuming a product form and one may also carry out calculations which employ Monte Carlo type sampling.) In the calculations reported below, we use a half-band width W of 32 and $\sigma/\Delta = 3.3$. *An important aspect of the DAF expressions for approximating a function and any of its derivatives at any point x is that they are completely unaffected by the fact that, used in a traditional manner, the Shannon–Gabor wavelet-DAF is not orthogonal.* In fact, in the theory of DAFs, it has been shown that the DAFs correspond to using a different basis for each point. The expansion coefficients are determined by a variational technique which turns out can be solved to arbitrarily high accuracy, so that one avoids having to compute the overlap matrix between different non-orthogonal functions [19,20,23]

We consider the time-dependent, incompressible fluid Navier–Stokes equation in the primitive variable formulation,

$$\frac{\partial \mathbf{V}}{\partial t} + \mathbf{V} \cdot \nabla \mathbf{V} = -\nabla p + \frac{1}{\text{Re}} \nabla^2 \mathbf{V} \quad \text{in } \Omega, \quad (5)$$

with the incompressibility condition,

$$\nabla \cdot \mathbf{V} = 0 \quad \text{in } \Omega. \quad (6)$$

Here, \mathbf{V} is the velocity field, p is the pressure, and Ω is the domain of the flow. We shall examine two separate boundary conditions, namely periodic (the Taylor problem) and the more usual requirement that the fluid velocity at the wall, $\mathbf{V} = \mathbf{V}|_{\partial\Omega}$, is equal to the local velocity of the wall. Since our primary emphasis is on the spatial discretization, we will use a simple

first order time approximation with a forward Eulerian scheme for the nonlinear convection and a backward Eulerian scheme for the diffusion [29]. That is (using standard notation),

$$\frac{\mathbf{V}^{n+1} - \mathbf{V}^n}{\Delta t} + \mathbf{V}^n \cdot \nabla \mathbf{V}^n = -\nabla p^{n+1/2} + \frac{1}{\text{Re}} \nabla^2 \mathbf{V}^{n+1} \quad \text{in } \Omega, \quad (7)$$

where $n + 1$ stands for the present time step. The pressure is treated as an intermediate force field and is approximated by the divergence of Eq. (7). This leads to a Poisson equation evaluated between the time steps

$$\nabla^2 p^{n+1/2} = f^n \quad \text{in } \Omega, \quad (8)$$

where

$$f^n = \frac{\nabla \cdot \mathbf{V}^n}{\Delta t} - \nabla \cdot (\mathbf{V}^n \cdot \nabla) \mathbf{V}^n. \quad (9)$$

The Poisson equation for pressure plays the role of the incompressibility condition (6) in the solution domain, provided that the boundary condition is satisfied [30]. As is well known, part of the difficulty in solving the incompressible Navier–Stokes equation is that both the governing equations and the boundary conditions are overspecified for the velocity field, and there is no unique governing equation and boundary condition for the pressure. Otherwise, the incompressible equation is easier to solve numerically than its compressible counterpart, because the latter has solutions containing possible shock waves and contact discontinuities.

In the present work, we employed wavelet-DAFs to achieve extremely high accuracy. This involves using the differentiating wavelet-DAF expression, Eq. (4), to convert the Eqs. (7) and (8) into inhomogeneous algebraic equations. Then one alternates between solving the algebraic equations arising from Eq. (7) and updating the pressure by solving Eq. (8). Next, one solves the algebraic equations due to Eq. (7), and so on. At each time step, we used matrix diagonalization to solve each of the two sets of inhomogeneous algebraic equations generated by the DAF-wavelet discretization of the Poisson-like equations (7) and (8). A wavelet-DAF-FFT solver for these equations, which will take advantage of the banded, Toeplitz structure of the DAF-wavelet matrices, is under development.

3. Applications

To illustrate the accuracy and robustness of the wavelet-DAF method for solving the incompressible Navier–Stokes equation, we consider two different numerical examples. Since one of the difficulties in solving the Navier–Stokes equation is associated with the boundary conditions, we chose to consider two different boundary conditions, namely, periodic and non-slip. The first example is the Taylor problem [33], which is analytically solvable. Thus, it provides an ideal test for various solution approaches [34,35].

The second example is the cavity flow, which is another commonly used benchmark problem for testing Navier–Stokes solvers [36–38]. Our DAF-wavelet results are presented in the following two subsections.

3.1. Periodic boundary conditions

We consider Eq. (5) in a square $[0, 2\pi] \times [0, 2\pi]$ with periodic boundary conditions in both dimensions. The initial values for the velocity vector $\mathbf{V} = (u, v)$ are taken to be

$$\begin{aligned} u(x, y, 0) &= -\cos(x) \sin(y), \\ v(x, y, 0) &= \sin(x) \cos(y), \end{aligned} \quad (10)$$

and obviously satisfy the incompressible condition $u_x + v_y = 0$. The analytical solutions are given by

$$\begin{aligned} u(x, y, t) &= -\cos(x) \sin(y) e^{-2t/\text{Re}}, \\ v(x, y, t) &= \sin(x) \cos(y) e^{-2t/\text{Re}}. \end{aligned} \quad (11)$$

Our calculations are conducted at a variety of Reynolds numbers ranging from $\text{Re} = 20$ to $\text{Re} = \infty$. A total of 32 grid points in an interval of $[0, 2\pi]$ in each dimension is used for testing the accuracy of our wavelet-DAF approach. The L_2 integration errors for four times ($t = 0.5, 1.0, 1.5, 2.0$) and various time meshes are listed in Table 1. The overall errors are extremely small due to the high accuracy of approximating spatial derivatives. The errors are shown to be clearly first order in the time discretization. The L_2 errors for various Reynolds numbers are listed in Table 2. Our results are much more accurate than those reported by E and Shu [34] using an “essentially non-oscillatory” scheme (ENO) with the same number of grid points. However, a detailed comparison

Table 1

L_2 errors of the numerical solutions for the Taylor problem ($\text{Re} = 1000, N = 32$)

Δt	$t = 0.5$	$t = 1.0$	$t = 1.5$	$t = 2.0$
0.1	3.23(-07)	6.46(-07)	9.68(-07)	1.29(-06)
0.05	1.62(-07)	3.23(-07)	4.84(-07)	6.45(-07)
0.01	3.23(-08)	6.46(-08)	9.66(-08)	1.29(-07)
0.005	1.62(-08)	3.23(-08)	4.84(-08)	6.45(-08)
0.001	3.23(-09)	6.46(-09)	9.68(-09)	1.29(-08)
0.0005	1.62(-09)	3.23(-09)	4.84(-09)	6.45(-09)
0.0001	3.27(-10)	6.53(-10)	9.78(-10)	1.30(-09)
0.00001	7.29(-11)	1.39(-10)	2.00(-10)	2.53(-10)

Table 2

L_2 errors of the numerical solutions for the Taylor problem ($\Delta t = 0.001, N = 32$)

Re	$t = 0.5$	$t = 1.0$	$t = 1.5$	$t = 2.0$
20	7.70(-06)	1.46(-05)	2.10(-05)	2.65(-05)
180	3.21(-07)	6.35(-07)	9.43(-07)	1.24(-06)
1000	3.23(-09)	6.46(-09)	9.68(-09)	1.29(-08)
10000	3.20(-11)	6.39(-11)	9.60(-11)	1.28(-10)
100000	7.01(-13)	1.39(-12)	2.24(-12)	3.28(-12)
∞	5.59(-15)	7.46(-15)	1.03(-14)	1.38(-14)

is not possible because these authors did not report the time meshes used in their integrations (as shown in Table 1, our approach reaches machine accuracy when the time mesh is sufficiently small). We also note that, although we use a grid spacing about three times larger than those used by Braza et al. [35], our wavelet-DAF results are substantially more accurate (they used a predictor–corrector pressure method, with a finite-volume second-order-accurate scheme and an alternating-direction-implicit procedure). It is interesting to note that the wavelet-DAF approach becomes even more accurate when the Reynolds number increases, reaching the computer limit of accuracy at $\text{Re} = \infty$. This observation has not been reported previously. This indicates that our wavelet-DAFs provide an extremely accurate spatial discretization for the incompressible Navier–Stokes equation.

3.2. Shear-driven cavity flow

Laminar flow in a square cavity, whose top wall moves with a uniform velocity in its own plane, has served as a model problem for testing and evaluat-

ing various numerical techniques for decades. On the one hand, the geometry of the problem is so simple that technical aspects can be easily compared in numerical tests. On the other hand, singularities occur at the corners of the model, which make it a nontrivial problem. In fact, there is an open question for this system about the possible appearance of a Hopf bifurcation at some critical values of the Reynolds number [39]. This has stimulated a new wave of both theoretical and numerical studies on the system. Whether such a bifurcation can indeed be detected by numerical methods is not altogether clear at this point due to the limited accuracy of conventional numerical techniques and limited computer capacity. Some results, obtained by spectral methods with regularized boundary conditions [40], gave strong indications that the continuous system could bifurcate to a periodic flow. However, additional studies, based on more accurate and reliable approaches, are required to draw a definitive conclusion. Our wavelet-DAF approach appears to be promising for resolving this open question. However, since the objective of the present work is simply to introduce our method for fluid dynamical problems, we shall not address this question in the present study.

The laminar incompressible cavity flow has singularities at its corners where high accuracy is required to describe the vortices. Gervais et al. [41] use a conformal image of the regular mesh by the mapping $X(i) = \sin^2(\frac{1}{2}\pi x(i))$, $Y(i) = \sin^2(\frac{1}{2}\pi y(i))$ to achieve better resolution at corner regions. As shown in the previous example, the wavelet-DAF discretization provides extremely high accuracy for spatial discretizations. This feature is utilized further in the present example by combining the wavelet-DAF accuracy with a somewhat different conformal mapping so as to achieve even greater accuracy with a smaller number of grid points. To this end we consider a transform in the domain of $[0, 1] \times [0, 1]$,

$$X(x) = \frac{1}{2 \tan A_x/2} [\tan A_x(x - \frac{1}{2}) + \tan A_x/2], \quad (12)$$

$$Y(y) = \frac{1}{2 \tan A_y/2} [\tan A_y(y - \frac{1}{2}) + \tan A_y/2], \quad (13)$$

where the mapping parameters $0 \leq A_x \leq \pi$ and $0 \leq A_y \leq \pi$ are used to adjust the grid density distribution in each dimension. In general, larger A_x and A_y

distribute more grid points in the corners, where they are needed for the cases of high Reynolds numbers. The boundary conditions are chosen as non-slip on three walls for both u and v ; u and v are symmetrically extended outside the walls so that their (fictitious) values in these regions can be used to estimate the derivatives near the boundaries. On the upper lid and beyond, v and u are set identically to 0 and 1, respectively. Neumann boundary conditions are used for the pressure.

Four different values of Reynolds numbers, 100, 400, 1000 and 3200, are considered in the present calculations, which used 63 or fewer grid points in each dimension, in contrast with the 129 points, in each dimension, typically used for this problem [36]. The time mesh used for all cases is $\Delta t = 0.002$. When $Re = 3200$, a total of 60 time units is used for the time integration. All other results are iterated up to 30 time units or fewer. We note that for relatively small Reynolds numbers, 100 and 400, convergence is attained in under 5 time units. Fig. 2 shows streamlines for the solutions subject to the above four Reynolds numbers. The streamline plots show a large primary vortex near the center of the cavity, along with two secondary vortices at the bottom corners. A shift of the center of the primary vortex toward the center of the cavity and a growth of the secondary vortices can be noted as the Reynolds number increases. The left and right asymmetry increases as the Reynolds number increases. This behavior is characteristic for this system.

4. Conclusion

We have numerically solved the incompressible Navier–Stokes equation, with two different boundary conditions, using our wavelet-DAF approach. The approach is shown to provide highly accurate results while using a relatively small number of grid points in solving the periodic Taylor problem (a standard problem for testing fluid dynamics methods). In particular, our results are much more accurate than the near-fourth-order, essentially non-oscillatory (ENO) scheme used by E and Shu. Only about a third of the number of grid points are required for our wavelet-DAFs to achieve the same accuracy as that obtained by Braza et al. [35] using their second order method.

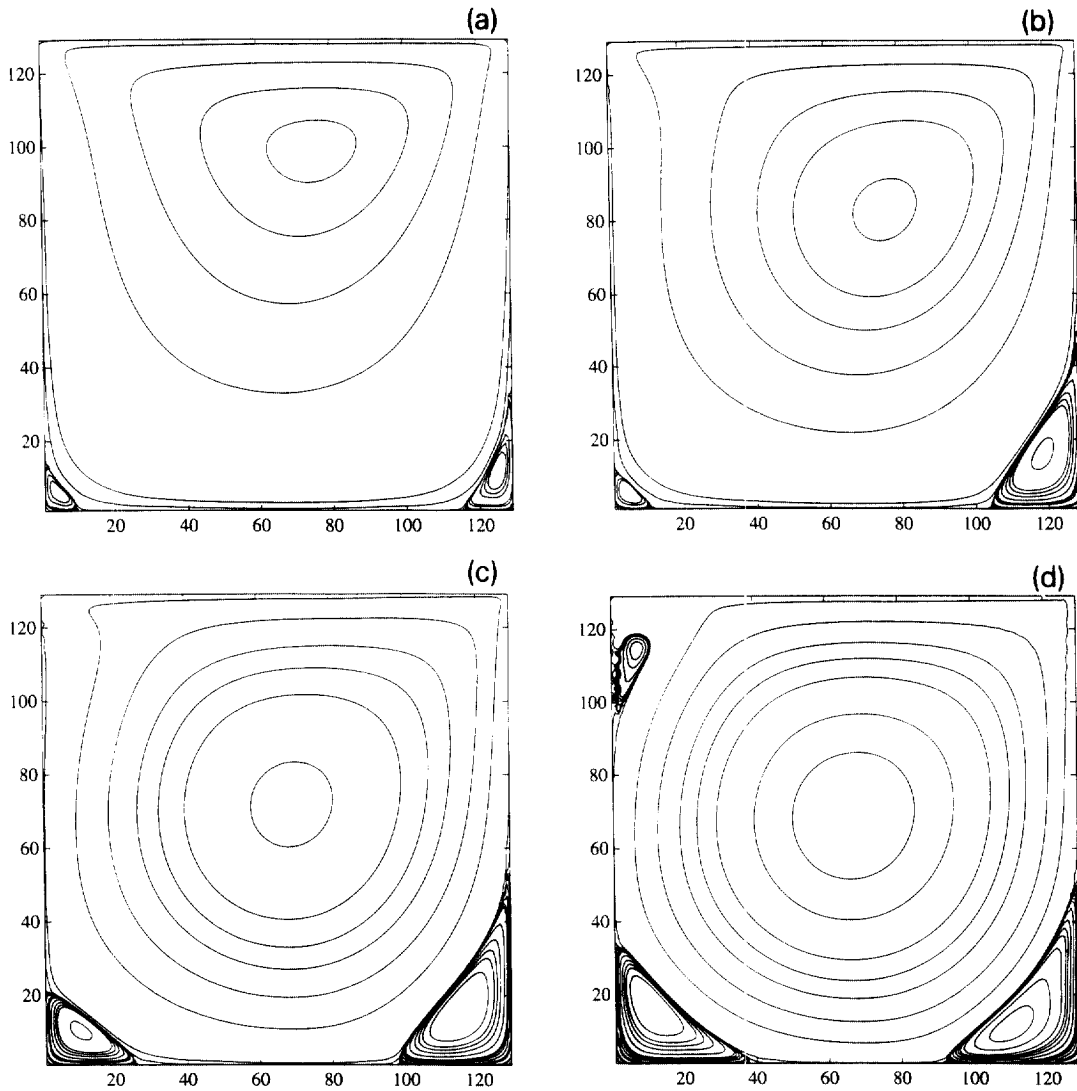


Fig. 2. The streamlines at different Re values: (a) $Re = 100$, $N = 52$, $A_x = 1.0$, $A_y = 1.0$; (b) $Re = 400$, $N = 54$, $A_x = 1.4$, $A_y = 1.0$; (c) $Re = 1000$, $N = 58$, $A_x = 2.0$, $A_y = 1.0$; (d) $Re = 3200$, $N = 63$, $A_x = 2.0$, $A_y = 1.2$. All results are plotted with a 129×129 grid.

In the case where the Reynolds number approaches infinity, our method yields results of machine accuracy. This is an indication of the superior accuracy of our wavelet-DAF approach for spatial discretizations. In our second example, a benchmark driven cavity problem, we integrate the system with 63 grid points or fewer, in each dimension, for Reynolds numbers as large as 3200. Results of similar accuracy have previously been obtained using 129 grid points in each spatial dimension [36]. The streamline plots

indicate that our results correctly describe the physics and are consistent with those of other authors [36]. Our results indicate that our wavelet-DAF approach offers significant advantages over conventional local methods in terms of accuracy, and that it is superior to existing global methods in its ability to handle boundary conditions. We believe that various wavelet-DAF methods can play an important role in fluid dynamical computations where singularities, such as vortex sheets, burst events and shock waves, can be present.

Acknowledgements

G.W.W. is supported under a postdoctoral fellowship from the NSERC of Canada, and is also supported in part under R.A. Welch Foundation Grant E-0608. D.S.Z. is supported under R.A. Welch Foundation Grant E-0608. S.C.A. is supported under National Science Foundation Grant CHE-9700297. D.J.K. is supported in part under National Science Foundation Grant CHE-9700297 and R.A. Welch Foundation Grant E-0608. The Ames Laboratory is operated for the Department of Energy by Iowa State University under Contract No 2-7405-ENG82.

References

- [1] L.P. Kadanoff, *Phys. Today* 50 (1997) 11.
- [2] M.J. Ablowitz, B.M. Herbst, C. Schober, *J. Comput. Phys.* 126 (1996) 299.
- [3] G. Beylkin, J.M. Keiser, *J. Comput. Phys.* 132 (1997) 233.
- [4] J. Fröhlich, K. Schneider, *J. Comput. Phys.* 130 (1997) 174.
- [5] R. Glowinski, T.W. Pan, R.O. Wells Jr., X. Zhou, *J. Comput. Phys.* 126 (1996) 40.
- [6] O.V. Vasilyev, S. Paolucci, *J. Comput. Phys.* 125 (1996) 498.
- [7] O.V. Vasilyev, S. Paolucci, M. Sen, *J. Comput. Phys.* 120 (1995) 33.
- [8] J.M. Restrepo, G.K. Leaf, *J. Comput. Phys.* 122 (1995) 118.
- [9] W.K. Liu, Y. Chen, *Int. J. Numer. Methods Fluids* 21 (1995) 901.
- [10] B. Jawerth, W. Swelden, *SIAM Rev.* 36 (1994) 377.
- [11] S. Qian, J. Weiss, *J. Comput. Phys.* 106 (1993) 155.
- [12] W. Dahmen, A. Kunoth, *Numer. Math.* 63 (1992) 315.
- [13] R.L. Schult, H.W. Wyld, *Phys. Rev. A* 46 (1992) 12.
- [14] Y. Meyer, *Wavelets and Operators*, Cambridge Stud. Adv. Math., Vol. 37 (Cambridge Univ. Press, Cambridge, 1992).
- [15] C.K. Chui, *An Introduction to Wavelets* (Academic Press, San Diego, 1992).
- [16] I. Daubechies, *Ten Lectures on Wavelets*, CBMS-NSF Series in Applied Mathematics (SIAM, Philadelphia, PA, 1992).
- [17] D.K. Hoffman, N. Nayar, O.A. Sharafeddin, D.J. Kouri, *J. Phys. Chem.* 95 (1991) 8299.
- [18] D.J. Kouri, W. Zhu, X. Ma, B.M. Pettitt, D.K. Hoffman, *J. Phys. Chem.* 96 (1992) 9622.
- [19] D.K. Hoffman, D.J. Kouri, in: *Proc. 3rd Int. Conf. on Math. & Num. Aspects of Wave Prop. Phenom.* (SIAM, Philadelphia, PA, 1995) pp. 56–83.
- [20] D.K. Hoffman, T.L. Marchioro II, M. Arnold, Y. Huang, W. Zhu, D.J. Kouri, *J. Math. Chem.* 20 (1996) 117.
- [21] G.W. Wei, D.S. Zhang, D.J. Kouri, D.K. Hoffman, *Phys. Rev. Lett.* 79 (1997) 775.
- [22] G.W. Wei, D.J. Kouri, D.K. Hoffman, *Computer Phys. Commun.*, in press.
- [23] D.K. Hoffman, G.W. Wei, D.S. Zhang, D.J. Kouri, *Chem Phys. Lett.* 287 (1998) 119; *Phys. Rev. E* 57 (1998) 6152.
- [24] G.W. Wei, D.J. Kouri, D.K. Hoffman, *Theor. Chem. Accounts*, in preparation.
- [25] G.W. Wei, S.C. Althorpe, D.J. Kouri, D.K. Hoffman, *J. Chem. Phys.* 108 (1998) 7065.
- [26] D.S. Zhang, G.W. Wei, D.J. Kouri, D.K. Hoffman, *Phys. Rev. E* 56 (1997) 1197; D.J. Kouri, D.S. Zhang, G.W. Wei, D.K. Hoffman, *Phys. Rev. E*, in press; G.W. Wei, D.S. Zhang, D.J. Kouri, D.K. Hoffman, *Comput. Phys. Commun.* 111 (1998) 87.
- [27] G.W. Wei, D.S. Zhang, D.J. Kouri, D.K. Hoffman, *Comput. Phys. Commun.* 111 (1998) 93.
- [28] G.W. Wei, S.C. Althorpe, D.S. Zhang, D.J. Kouri, D.K. Hoffman, *Phys. Rev. A* 57 (1998) 3309.
- [29] H.H. Yang, B.R. Seymour, B.D. Shizgal, *Computers Fluids* 23 (1994) 829.
- [30] S. Adjerid, J.E. Flaherty, *SIAM J. Numer. Analysis* 23 (1986) 778.
- [31] P. Le Quééré, T. Alziary de Roquefort, *J. Comput. Phys.* 57 (1985) 210.
- [32] A. Harten, B. Engquist, S. Osher, S. Chakravarthy, *J. Comput. Phys.* 71 (1987) 231.
- [33] See, for example, *The Collected Works of G.I. Taylor*, Vol. 2, G.K. Batchelor, ed. (Cambridge Univ. Press, Cambridge).
- [34] W. E, C.W. Shu, *J. Comput. Phys.* 110 (1994) 39.
- [35] M. Braza, P. Chassaing, H.H. Minh, *J. Fluid Mech.*, 165 79 (1986).
- [36] U. Ghia, K.N. Ghia, C.T. Shin, *J. Comput. Phys.* 48 (1982) 387.
- [37] R. Schreiber, H.B. Keller, *J. Comput. Phys.* 49 (1983) 310.
- [38] J.-L. Guermond, L. Quartapelle, *J. Comput. Phys.* 132 (1997) 12.
- [39] J.W. Goodrich, K. Gustafson, K. Halasi, *J. Comput. Phys.* 90 (1990) 219.
- [40] J. Sher, *J. Comput. Phys.* 95 (1991) 228.
- [41] J.J. Gervais, D. Lemelin, R. Pierre, *Int. J. Numer. Methods Fluids* 24 (1997) 477.